SPE 122456

Conceptualization and Modeling of Flow and Transport Through Fault Zones

Yu-Shu Wu, SPE, Colorado School of Mines, and Kenzi Karasaki, Lawrence Berkeley National Laboratory

This paper was prepared for presentation at the 2009 SPE Latin American and Caribbean Petroleum Engineering Conference held in Cartagena, Colombia, 31 May–3 June 2009.

Abstract

A physically based fault conceptual model is presented for modeling multiphase flow and transport processes in fractured rock of fault zones. In particular, we discuss a general mathematical framework model for dealing with fracture-matrix interactions, which is applicable to both continuum and discrete fracture conceptualization in fault zones. In this conceptual model, faults or fault zones of formations are conceptualized as a multiple-continuum medium, consisting of (1) highly permeable, large-scale and well-connected fractures, (2) low-permeability rock matrix, (3) various-sized vugs or large pore volumes, and (4) surrounding fractured or matrix formations on both sides. Flow through fault zones may be different from that through fractured reservoir rock, because of higer permeabilities and larger pore spaces in fault zones. In addition fault flow may be further complicated by non-Darcy's and other nonlinear flow behavior because of large pore space. To account for such complicated flow regime, our model formulation includes non-Darcy flow, using the multiphase extension of the *Forchheimer* equation as well as descriptions for flow in parallel-wall fractures or tubes, based on solutions of flow through a parallel-wall, uniform fracture and Hagen-Poiseuille tube flow.

The proposed fault flow model is discretized using an unstructured grid with regular or irregular meshes, followed by time discretization carried out using a backward, first-order, finite-difference method. The final discrete nonlinear equations are handled fully implicitly, using Newton iteration. The numerical scheme proposed is applicable to simulating multiphase fluid and heat flow as well as solute transport through the fractured fault zones and their interaction with surrounding rocks. The conceptual fault model is implemented into a general-purpose reservoir simulator, applicable to 1-D, 2-D, and 3-D simulation of multiphase flow in fault zones. As a demonstration example, we apply the model to simulate pressure and temperature responses in wells for a flow system controlled by faults.

Introduction

Since the 1960s, a number of numerical approaches and techniques have been developed and applied for modeling flow and transport processes in fractured reservoirs (e. g., Kazemi, 1969; Pruess and Narasimhan, 1985; Wu and Pruess, 1988). Even with the significant progress has been made towards understanding and modeling of flow and transport processes in fractured rock so far, most studies have focused primarily on naturally fractured reservoirs without taking into consideration of faults explicitly. Recently, characterizing fractured rock of faults or fault zones has received attention, because fault zones are found to be closely associated with and may dominate flow and transport processes in fractured reservoirs (Wu et al. 2004; 2006a; 2007a).

Mathematical approaches developed for modeling flow through fractured reservoirs rely in general on continuum approaches, involving developing conceptual models, incorporating the geometrical information of a given fracture-matrix system, setting up mass and energy conservation equations for fracture-matrix domains, and then solving discrete nonlinear algebraic equations of mass and energy conservation. The commonly used mathematical methods for modeling flow through fractured rock include: (1) an explicit discrete-fracture and matrix model (Snow, 1965), (2) a dual- and multiple-continuum method, including double- and multi-porosity, dual-permeability, or the more general "multiple interacting continua" (MINC) method (Warren and Root, 1963; Kazemi, 1969; Pruess and Narasimhan, 1985; Wu and Pruess, 1988), and (3) an effective-continuum method (ECM) (Wu, 2000).

In addition to the traditional double-porosity concept, a number of triple-porosity or triple-continuum models have been proposed (Closemann, 1975; Wu et al. 2004a; Kang et al. 2006; Wu et al. 2007b) to describe flow through fractured rocks. In particular, Liu et al. (2003) and Camacho-Velazquez et al. (2005) present several new triple-continuum models for single-phase flow in a fracture-matrix system that include cavities within the rock matrix (as an additional porous portion of the

matrix). In general, these models have focused on handling the heterogeneity of the rock matrix or fractures, e.g., subdividing the rock matrix or fractures into two or more subdomains with different properties. In concept, all these approaches can be applied to modeling flow and transport in highly densed fractures in fault zones.

Dual-continuum or multiple-continuum approaches, as applied in this study, include the classical double-porosity model (Barenblatt et al. 1960; Warren and Root, 1963) , the dual-permeability concept, and the more rigorous dual-continuum generalization of the MINC (Pruess and Narasimhan, 1985) and the multicontinuum model (Wu and Pruess, 1988) for modeling flow in fractured porous media. In the double-porosity model, a flow domain is composed of matrix blocks with low permeability, embedded in a network of interconnected fractures. Global flow and transport in the formation occur only through the fracture system, conceptualized as an effective continuum. This model treats matrix blocks as spatially distributed sinks or sources to the fracture system without accounting for global matrix-matrix flow. In comparison, the MINC concept is able to describe gradients of pressures, temperatures, or concentrations near matrix surface and inside the matrix—by further subdividing individual matrix blocks with one- or multidimensional strings of nested meshes. Therefore, the MINC model in general provides a better numerical approximation for transient fracture-matrix interactions than the double-porosity model. Because of its computational efficiency and its ability to match many types of observed data of fields with fault flow (e.g., Wu et al. 2004; 2007a), the dual-continuum models, as in the double-porosity and dual-permeability concepts, has perhaps been the most widely used method in petroleum and geothermal engineering, as well as in groundwater hydrogeology, and will be used for this study.

In this paper, a physically based fault conceptual model is presented for modeling multiphase flow and transport processes in fractured rock of fault zones. In particular, we discuss a general mathematical framework model for dealing with fracture-matrix interactions, which is applicable to both continuum and discrete fracture conceptualization in fault zones. The multi-continuum, physically based conceptual mathematical model to include the effects of various scaled fractures, vugs or cavities on water and heat flow processes in fault zones. In this continuum model, faults or fault zones of formations is conceptualized as a multiple-continuum medium, consisting of (1) highly permeable, large-scale and well-connected fractures, (2) low-permeability rock matrix, and (3) various-sized vugs (if existing). Similar to the conventional double-porosity model, the large-scale, well connected fracture continuum is responsible for global flow within faults, while vuggy and matrix continua, providing storage space, are locally connected to each other (and interacting with globally connecting fractures). In addition, the flow long faults is also interacting laterally with formations layer on both sides of the fault zones.

In this approach, a subsurface fault domain, consisting of fractures, rock matrix, vugs, or other large pores, is discretized using an unstructured grid with regular or irregular meshes, followed by time discretization carried out using a backward, first-order, finite-difference method. The final discrete nonlinear equations are handled fully implicitly, using Newton iteration. In addition, the fracture medium is handled using a general dual-continuum concept with continuum or discrete modeling approaches. We demonstrate that with this unified approach, modeling a particular process of fracture- or porous-medium flow and transport in fault zones becomes simply a matter of defining types of media (i.e., fractures, matrix, vugs, or other large pores) with a set of state variables, along with their interactions on the interfaces between continua. This numerical scheme proposed is applicable to simulating water and heat flow as well as solute transport through the fractured fault zones and their interaction with surrounding rock layers.

Conceptual Model of Fractured Faults

Faults may consist of a single fracture or multiple, various scale fractures, or highly- densed fractured zones. In general, faults or fault zones belong to typical fractured rock and can be classified as a special case of fractured reservoirs. A typical fractured reservoir consists of large-scale fractures, low-permeable rock matrix, and a number of various sized cavities or vugs. Figure 1 shows a formation of outcrops with a vertical fault (Wu et al. 2006b), and the fractured system is conceptualized using vertical and horizontal fracture network with vugs along the vertical fault in the figure.

Different types of fractured rock in fault zones can be described using a multi-continuum concept. The multi-continuum conceptual model considers large fractures as main pathways for the global flow. Vuggy and matrix continua, locally connected to each other as well as directly or indirectly interacting with globally connecting fractures, provide storage space as sinks or sources to fractures. Note that vugs directly connected with fractures could be considered part of the fracture continuum. More specifically, we conceptualize the fractured-vug-matrix system of fault zones as consisting of (1) fracture continuum: “large” fractures (or fractures), *globally connected* on the scale of model domains, providing flow paths to injection and production wells; (2) vuggy continuum: various-sized vugs or large pore space cavities, which are *locally connected* to fractures either through “small” fractures or *isolated* by rock matrix; (3) matrix continuum: rock matrix, which may contain a number of cavities, *locally connected* to large fractures and/or to vugs; and (4), small-scale fractures (Wu et al. 2004a).

In principle, the proposed multiple-continuum model for fault zones is a natural extension of the generalized multiple-continuum (MINC) approach (Pruess and Narasimhan, 1985; Wu and Pruess, 1988). In this approach, an “effective” porous medium is used to an approximate fractures, vugs (if any), rock matrix continuum, or any large pores. The triple- or multiple-continuum conceptual model assumes that approximate thermodynamic equilibrium exists locally within each of the continua at all times. Based on this local equilibrium assumption, we can define thermodynamic variables, such as pressure, fluid saturation, concentration, and temperature, for each continuum. Note that the multiple-continuum model is not limited to the orthogonal idealization of the fracture system, or uniform size, regular shape, or distribution of vugs and cavities, as

illustrated in Figure 1. Irregular and stochastic distributions of fractures and cavities can be handled numerically, as long as the actual distribution patterns are known (Pruess, 1983).

Mathematical Model

The physical processes associated with flow and transport in fractured porous media in fault zones are governed by the same fundamental conservation laws as those used in other branches of the sciences and engineering: conservation of mass, momentum, and energy governs the behavior of fluid flow, chemical transport, and heat transfer in porous or fractured rock. These physical laws are often represented mathematically on the macroscopic level by a set of partial differential or integral equations, called governing equations. These governing equations are generally nonlinear, as long as compressible fluid flow or heat transfer is involved and needed to quantitatively model the flow and transport processes occurring in porous or fractured media. Based on the general conservation laws, we present a set of generalized governing equations for fluid flow, multicomponent transport, and heat transfer in porous and fractured media, providing a framework for numerical formulations to cover all possible scenarios for flow and transport in porous media.

We consider the following physical processes in fault zones: (1) single-phase aqueous phase flow, (2) solute (multiple minerals) transport, and (3) ambient heat flow, driven by geothermal gradient. Let us consider a nonisothermal system consisting of one aqueous fluid phase, which in turn consists of a number of mass components. To derive a set of generalized governing equations for fluid flow, multicomponent transport, and heat transfer, we assume that these processes can be described using a continuum approach within a representative elementary volume (REV) in a porous or fractured medium. In addition, a condition of local thermodynamic equilibrium is assumed, so that at any time temperatures, phase pressures, densities, viscosities, enthalpies, internal energies, and component concentrations (or mass fractions) are the same locally at each REV of the porous medium.

According to mass and energy conservation principles, a generalized conservation equation of mass components and energy in the porous continuum can be written as follows:

$$\frac{\partial M^k}{\partial t} = G^k + q^k + F^k \tag{1}$$

where superscript k is the index for the components, k = 1, 2, 3,…, N_c, with N_c being the total number of mass components and with k = N_c+1 for an energy "component" (note that heat energy is here regarded as a component for convenience); M is the accumulation term of component k; G^k is the decay or internal generation (reaction) term of mass or energy components; q^k is an external source/sink term or fracture-matrix exchange term for mass or energy component k and energy; and F^k is the "flow" term of mass or energy movement or net exchange from single-phase flow, or diffusive and dispersive mass transport, or heat transfer, as discussed below.

In addition to the conservation or continuity equations of mass and thermal energy, shown in Equation (1), we also need specific relationships or *mechanisms* that describe why and how fluid flow, solute transport, and heat transfer occur in porous and fractured media. This is to define the "flow" term in Equation (1), and the following specific laws act as such mechanisms by governing local fluid flow, component transport, and heat transfer processes in porous media.

Single-Phase Darcy Flow: For single-phase liquid flow, the accumulation terms in Equation (1) for water phase is evaluated as

$$M^w = \rho_w \phi \tag{2}$$

where ρ_w is the density of water phase; and ϕ is the porosity of porous or fractured media. Note that in this special case, the decay or generation term is negligible with

$$G^w = 0 \tag{3}$$

The mass flow term is determined by

$$F^w = \nabla \bullet (\rho_w \mathbf{v}_v) \tag{4}$$

where $\mathbf{v}_w$ is a vector of the Darcy's velocity or volumetric flow of water, defined by Darcy's law to describe the flow of single fluid as

$$\mathbf{v}_w = -\frac{k}{\mu}(\nabla P_w - \rho_w g \nabla z) \tag{5}$$

where P_w, μ, and g are pressure, viscosity of water phase, and gravitational constant, respectively; z is the vertical coordinate; k is absolute or intrinsic permeability (a tensor in general).

Mass Transport: The movement of dissolved mass components or chemical species in a fluid-rock medium system can also be handled as a special case of Equation (1). The accumulation terms for component k is

$$M^k = \phi \rho_w X_w^k + (1-\phi)\ \rho_s \rho_w X_w^k K_d^k \quad (k = 1, 2, 3,\ldots, N_c) \tag{6}$$

where X_w^κ is the mass fraction of component k in water; ρ_s is the density of rock solids; and K_d^k is the distribution coefficient of component k between the aqueous phase and rock solids to account for adsorption effects.

In the case in which components are subject to a first-order radioactive decay, the decay/generation term is

$$G^k = \phi\lambda_k\left(\rho_w X_w^k + (1-\phi)\,\rho_s\,\rho_w\,X_w^k\,K_d^k\right) \quad (k = 1, 2, 3,\ldots, N_c) \tag{7}$$

where λ_k is the radioactive decay constant of component k.

The mass component transport is governed in general by processes of advection, diffusion, and dispersion, and is also subject to other processes such as radioactive decay, adsorption, dissolution and precipitation, mass exchange and partition between phases, or chemical reactions. Advective transport of a component or solute is carried by flow of a fluid, and diffusive and dispersive flux is contributed by molecular diffusion and mechanical dispersion, or hydrodynamic dispersion. These processes are described using a modified Fick's law for transport through a single-phase porous medium (Wu, 2000a). Then, the total mass flow term for a component k, by advection and dispersion, is written as

$$F^k = -\nabla\bullet\left(\rho_w\,X_w^k\,\mathbf{v}_w\right) + \underline{D}_w^k\bullet\nabla\left(\rho_w X_w^k\right) \quad (k = 1, 2, 3,\ldots, N_c) \tag{8}$$

Equation (8) indicates that the mass flow consists of two parts, the first part, i.e., the first term on the right-hand side of (8), is contributed by advection in water flow, and the second part [the second term on the right-hand side of (8)] is diffusive flux by hydrodynamic dispersion. In Equation (8), $\underline{D}_w^k$ is the hydrodynamic dispersion tensor accounting for both molecular diffusion and mechanical dispersion for component k in water phase, defined by an extended dispersion model (Scheidegger, 1961),

$$\underline{D}_w^k = \alpha_T|\mathbf{v}_w|\delta_{ij} + (\alpha_L - \alpha_T)\frac{\mathbf{v}_w\mathbf{v}_w}{|\mathbf{v}_w|} + \phi\tau\,d_w^k\delta_{ij} \quad (k = 1, 2, 3,\ldots, N_c) \tag{9}$$

where α_T and α_L are transverse and longitudinal dispersivities, respectively, in water phase of porous or fractured media; τ is tortuosity of the porous medium; d_w^k is the molecular diffusion coefficient of component k within water phase; and δ_{ij} is the Kronecker delta function ($\delta_{ij} = 1$ for i = j, and $\delta_{ij} = 0$ for $i \neq j$), with i and j being coordinate indices.

Heat Transfer: The accumulation term for the heat equation is usually is defined as

$$M^{N_c+1} = \phi\,\rho_w U_w + (1-\phi)\,\rho_s\,U_s \tag{10}$$

where U_β and U_s are the internal energies of water phase and rock solids, respectively.

Heat transfer in porous and fractured media is in general a result of both convective and conductive processes. Heat convection is contributed by thermal energy carried mainly by bulk flow of water. On the other hand, heat conduction is driven by temperature gradients and may follow Fourier's law. Then the combined, overall heat flux term, owing to convection, conduction and radiation in a multiphase, multicomponent, porous medium system, may be described as

$$F^{N_c+1} = -\nabla\bullet\left(h_w\,\rho_w\,\mathbf{v}_w\right) + \nabla\bullet\left(K_T\nabla T\right) \tag{11}$$

where h_w is specific enthalpies of water phase K_T is the overall thermal conductivity; and T is temperature;

Constitutive Relationships: To complete the mathematical description of water flow, multicomponent transport, and heat transfer in porous and fractured media, Equation (1), a generalized mass- and energy-balance equation, needs to be supplemented with a number of constitutive equations. These constitutive correlations express interrelationships and constraints of physical processes, variables, and parameters, and allow the evaluation of secondary variables and parameters as functions of a set of primary unknowns or variables selected to make the governing equations solvable. Many of these correlations for estimating properties and interrelationships are determined by experimental studies.

Numerical Formulation and Solution

The methodology for using numerical approaches to simulate subsurface flow and transport, and heat transfer, consists in general of the following three steps: (1) spatial discretization of mass and energy conservation equations, (2) time discretization; and (3) iterative approaches to solve the resulting nonlinear, discrete algebraic equations. Among various numerical techniques for simulation studies, a mass- and energy-conserving discretization scheme, based on finite or integral finite-difference or finite-element methods, is the most commonly used approach and is discussed here.

Discrete Equations: The component mass- and energy-balance Equation (1) are discretized in space using a control-volume concept. The control-volume approach provides a general spatial discretization scheme that can represent a one-, two- or three-dimensional domain using a set of discrete meshes. Each mesh has a certain control volume for a proper averaging or interpolation of flow and transport properties or thermodynamic variables. The control volume concept includes the conventional finite-difference scheme (Aziz and Settari, 1979; Narasimhan and Witherspoon 1976; Pruess et al. 1999) an integral finite-difference method (Figure 2), a control-volume finite element (Forsyth, 1994), and Galerkin finite-element

methods (Huyakorn et al. 1994). These are the most widely used discretization schemes for subsurface flow and transport simulation.

As shown in Figure 2, the spatial discretization of Equation (1) is carried out using the integrated finite difference scheme, and time discretization is carried out using a backward, first-order, fully implicit finite-difference scheme. The discrete nonlinear equations for components of water, other mass components, and heat at gridblock or node i can be written in a general form:

$$\left\{M_i^{k,n+1} + G_i^{k,n+1}\Delta t - M_i^{k,n}\right\}\frac{V_i}{\Delta t} = \sum_{j\in\eta_i} flow_{ij}^{k,n+1} + Q_i^{k,n+1} \qquad (12)$$

$$(k = 1, 2, 3, \ldots, N_c, N_c+1) \text{ and } (i=1, 2, 3, \ldots, N)$$

where superscript k serves also as an equation index for all mass components with k = 1, 2, 3, …, N_c and k = N_c+1 denoting the heat equation; superscript n denotes the previous time level, with n+1 the current time level to be solved; subscript i refers to the index of gridblock or node i, with N being the total number of nodes in the grid; Δt is time step size; V_i is the volume of node i; η_i contains the set of direct neighboring nodes (j) of node i; A_i^k, G_i^k, $flow_{ij}^k$, and Q_i^k are the accumulation and decay/generation terms, respectively, at node i; the "flow" term between nodes i and j, and sink/source term at node i for component k or thermal energy, respectively, are defined below. Equation (12) has the same form regardless of the dimensionality of the system, i.e., it applies to one-, two-, or three-dimensional flow, transport, and heat-transfer analyses within and outside of fault zones.

The accumulation and decay/generation terms for mass components or thermal energy are evaluated using Equations (6), (7), and (10), respectively, at each node i. The "flow" terms in Equation (12) are generic and include mass fluxes by advective and dispersive processes, as described by Equation (4) or (8), as well as heat transfer, described by (11). The mass flow term of Equation (12) for single-phase water flow is described by a discrete version of Darcy's law, i.e., the mass flux of water phase along the connection is given by

$$flow_{ij}^w = \lambda_{w,ij+1/2}\gamma_{ij}\left[\psi_j - \psi_i\right] \qquad (13)$$

where $\lambda_{w,i\,j+1/2}$ is the mobility term to water phase, defined as

$$\lambda_{w,i\,j+1/2} = \left(\frac{\rho_w}{\mu}\right)_{ij+1/2} \qquad (14)$$

In Equation (13), γ_{ij} is transmissivity and is defined differently for finite-difference or finite-element discretization. If the integral finite-difference scheme (Pruess et al. 1999) is used, the transmissivity is evaluated as

$$\gamma_{ij} = \frac{A_{ij}k_{i\,j+1/2}}{D_i + D_j} \qquad (15)$$

where A_{ij} is the common interface area between connected blocks or nodes i and j (Figure 3); and D_i is the distance from the center of block i to the interface between blocks i and j (Figure 3). The flow potential term in Equation (13) is defined as

$$\psi_i = P_{w\,i} - \rho_{w,ij+1/2}\, g\, Z_i \qquad (16)$$

where Z_i is the depth to the center of block i from a reference datum.

For mass component transport, the flow term, or the net mass flux by advection and hydrodynamic dispersion of a component along the connection of nodes i and j, is determined by

$$flow_{ij}^k = F_{A,ij}^k + F_{D,ij}^k \quad (k = 1, 2 , 3, \ldots, N_c) \qquad (17)$$

where $F_{A,ij}^k$ and $F_{D,ij}^k$ are the net mass fluxes by advection and hydrodynamic dispersion along the connection, respectively, with

$$F_{A,ij}^k = A_{ij}\left(X_\beta^k\right)_{ij+1/2} flow_{i\,j}^w \qquad (18)$$

and

$$F_{D,ij}^k = -\mathbf{n}_{ij} \bullet A_{ij}\underline{D}_w^k \bullet \nabla\left(\rho_w X_w^k\right) \qquad (19)$$

where $\mathbf{n}_{ij}$ is the unit vector along the connection of the two blocks i and j.

The total heat flux along the connection of nodes i and j, including advective and conductive terms, can be also evaluated, when using a finite-difference scheme, by

$$flow_{ij}^{N_c+1} = \left(h_w\right)_{ij+1/2} flow_{i\,j}^w + A_{ij}\left(K_T\right)_{ij+1/2}\left[\frac{T_j - T_i}{D_i + D_j}\right] \qquad (20)$$

In evaluating the "flow" terms in the above Equations (13)–(16), (18), and (20), subscript ij+1/2 is used to denote a proper averaging or weighting of fluid flow, component transport, or heat-transfer properties at the interface or along the connection between two blocks or nodes i and j. The convention for the signs of flow terms is that flow from node j into node i is defined as "+" (positive) in calculating the flow terms. Wu and Pruess (2000a) present a general approach to calculating these flow terms associated with advective and dispersive mass transport and heat transfer in a multiphase system, using an irregular and unstructured, multidimensional grid.

The mass or energy sink/source in Equation (12) at node i, Q_i^k, is defined as the mass or energy exchange rate per unit volume of rock or soils. It is normally used to treat boundary conditions, such as surface infiltration, pumping, and injection through wells.

Note that we present explicit, discrete expressions for estimating all the flow terms above, except for dispersive fluxes in Equation (18). This is because of the numerical difficulties introduced in handling the hydrodynamic tensor of dispersion, which is treated very differently with different numerical approaches, such as finite difference or finite element. In most formulations for solute transport, the off-diagonal terms and contributions of the dispersion tensor are ignored, and dispersive transport is considered only along the principal directions. However, a general procedure for using the integral finite difference to incorporate a full dispersion tensor is presented by Wu and Pruess (2000a).

Equation (12) presents a precise form of the balance equation for each mass component and heat in a discrete form. It states that the rate of change in mass or energy accumulation (plus decay/generation, if existing) at a node over a time step is exactly balanced by inflow/outflow of mass and energy, and also by sink/source terms, when existing for the node. As long as all flow terms have flow from node i to node j equal to and opposite to that of node j to node i for fluids, components, and heat, no mass or energy will be lost or created in the formulation during the solution. Therefore, the discretization in (12) is conservative.

Non-Darcy's and Other Complicated Flow

Flow regime may be more complicated within faults or fault zones, because of (1) the high permeability of fractures and (2) large pores, such as vugs and larger-aperture fractures, in fault zones.

No-Darcy Flow: In addition to Darcy flow, as described in Equations (5) or (13), non-Darcy flow may also occur between and among the multiple continua within fault zones. A general numerical approach for modeling non-Darcy flow (Wu, 2002) can be directly extended to the multiple-continuum model of this work for flow in fault zones. Volumetric flow rate (namely Darcy velocity for Darcy flow) for non-Darcy flow of each fluid may be described using the multiphase extension of the *Forchheimer* equation:

$$-\left(\nabla P_w - \rho_w \mathbf{g}\right) = \frac{\mu}{k}\mathbf{v}_w + \beta\rho_w \mathbf{v}_w\left|\mathbf{v}_w\right| \tag{21}$$

β is the non-Darcy flow coefficient, intrinsic rock property, with a unit m^{-1} for water phase under flow condition.

Note that no mater what type the flow, i.e., Darcy's flow, non-Darcy's flow, or the following pipe-type flow, the discrete mass and energy balance equation of (12) is always valid. For the case of non-Darcy's flow, the flow term (flow_{ij}^{w}) in Equation (13) along the connection (i, j), between elements i and j, is numerically replaced by (Wu, 2002),

$$\mathrm{flow}_{ij}^{w} = \frac{A_{ij}}{2(k\beta)_{ij+1/2}}\left\{-\frac{1}{\lambda_\beta} + \left[\left(\frac{1}{\lambda_\beta}\right)^2 - \bar{\gamma}_{ij}\left(\psi_{\beta j} - \psi_{\beta i}\right)\right]^{1/2}\right\} \tag{22}$$

$$\bar{\gamma}_{ij} = \frac{4\left(k^2\rho_w\beta\right)_{ij+1/2}}{D_i + D_j} \tag{23}$$

Flow in Parallel-Wall Fracture or Tube: In general, flow along connecting paths of large-aperture fractures or vugs through narrow pores or fractures may be too fast or openings are too large to describe using Darcy's law. In particular, when these large-aperture fractures vuggy connections could be approximated as a single (or parallel) fracture or tube within fault zones, solutions of flow through a parallel-wall, uniform fracture or Hagen-Poiseuille tube-flow solution (Bird et al., 1960) may be extended to describe such flow in Equation (13):

$$\gamma_{ij} = \frac{wb^3}{12\left(D_i + D_j\right)} \qquad \text{for fracture-type connection} \tag{24}$$

and

$$\gamma_{ij} = \frac{\pi r^4}{8\left(D_i + D_j\right)} \qquad \text{for tube-type connection} \tag{25}$$

where b is fracture aperture, w is fracture width, and r is tube radius. Similarly, flow solutions for both laminar and turbulent flow through simple geometry of vug-vug connections can be used for flow between these vuggy connections.

Effect of Rock Deformation: Based on the observation from experimental results (Wu et al. 2008) and previous research (Terzaghi, 1943), the effective porosity and permeability of porous and fractured rock in an isothermal system are assumed to correlate with the mean effective stress (σ'_m), defined as:

$$\sigma'_m = \sigma_m(x, y, z, P_w) - \alpha P_w \tag{26}$$

where σ_m is mean total stress; α is Biot's effective parameter (Biot, 1941), and is treated as constant at space or in general estimated by

$$\sigma_m(x,y,z,P_w)=(\sigma_x(x,y,z,P)+\sigma_y(x,y,z,P)+\sigma_z(x,y,z,P_w))/3 \tag{27}$$

where σ_x, σ_y, and σ_z are total stress in x, y, and z- directions, respectively.

With the definition of the mean effective stress of Equation (26), the effective porosity of fractures and rock matrix in fault zones is defined as a function of mean effective stress only,

$$\phi = \phi(\sigma'_m) \tag{28}$$

Similarly, intrinsic permeability is related to the effective stress as,

$$k = k(\sigma'_m) \tag{29}$$

To incorporate rock-deformation effects at a given site, the proposed models, derived from Equations (28) and (29), need to be determined from laboratory or field studies. The key for applicability of these models, in fault flow simulations coupled with rock deformation, is that the distribution of effective stress or total stress field must be predetermined as a function of spatial coordinates and pressure fields, as in Equations (26) and (27). In practice, the stress distribution may be estimated analytically, numerically, or from field measurements, because changes in effective stress are primarily caused by changes in pressure in reservoirs.

When the functions of (28) and (29) are determined, then the two equations are used in flow and transport calculations. For example, Equation (28) is used in (6) and (10) for accumulation terms, while (29) is used in (13) or (22) for flow calculation to incorporate effect of rock deformation of fault flow.

Handling Fracture-Vug-Matrix Interaction in Faults

The technique used in this work for handling flow through vuggy fractured rock follows the dual- or multiple-continuum methodology (Warren and Root, 1963; Pruess and Narasimhan, 1985; Wu and Pruess, 1988). With this dual-continuum concept, equations for fluid and heat flow and mass transport discussed above can be used to describe flow along fractures and inside matrix blocks, as well as fracture-matrix-vug interaction. However, special attention needs to be paid to interporosity flow in the fracture-matrix-vug continua. Flow terms of interporosity between fracture-matrix, fracture-vug, vug-vug, and vug-matrix connections are all evaluated using Equation (13) or (22). However, the transmissivity of (15) will be evaluated differently for different types of interporosity flow. For fracture-matrix Darcy flow, γ_{ij}, is given by (Wu et al. 2006b).

$$\gamma_{FM} = \frac{A_{FM} k_M}{l_{FM}} \tag{30}$$

where A_{FM} is the total interfacial area between fractures (F) and the matrix (M) elements; k_M is the absolute matrix permeability; and l_{FM} is the characteristic distance for flow crossing fracture-matrix interfaces. For fracture-vug flow, γ_{ij} is defined as

$$\gamma_{FV} = \frac{A_{FV} k_V}{l_{FV}} \tag{31}$$

where A_{FV} is the total interfacial area between the fracture and vugs (V) elements; l_{FV} is a characteristic distance for flow between fractures and vugs; and k_V is the absolute vuggy permeability, which should be the permeability of small fractures that control flow between vugs and fractures. Note that for the domain in which vugs are isolated from fractures, no fracture-vug flow terms need to be calculated, because they are indirectly connected through the matrix.

For vug-matrix flow, γ_{ij} is evaluated as

$$\gamma_{VM} = \frac{A_{VM} k_M}{l_{VM}} \tag{32}$$

where A_{VM} is the total interfacial area between the vug and matrix elements; and l_{VM} is a characteristic distance for flow crossing vug-matrix interfaces. Similarly, the transmissivity between vugs, when they are connected through narrow fractures or tube can be defined.

Note that Table 1 summarizes several simple models for estimating characteristic distances in calculating inter-porosity flow within fractures, vugs, and the matrix. In such cases, we have regular one-, two-, or three-dimensional large fracture networks, each with uniformly distributed small fractures connecting vugs or isolating vugs from fractures, based on the quasi-steady-state flow assumption of Warren and Root (1963). In practical application of the proposed modeling approach, the MINC concept (Pruess, 1983; Pruess and Narasimhan, 1985) is extended to modeling flow through fractured-vuggy rock. In this approach, we start with a primary or single-continuum medium mesh that uses bulk volume of formation and layering data. Then, geometric information for the corresponding fractures and vugs within each formation subdomain of fault zones and their surrounding rock is used to generate integrated finite-difference meshes from the primary grid. Figure 3 shows a methodology used for represeting a three-dimensional grid of a fault zone in a primary mesh (Pan et al. 2000). Then, based on the the primary mesh, fractures are lumped together into the fracture continuum, while vugs with or without small fractures are lumped together into the vuggy continuum. The rest is treated as the matrix continuum. Connection distances and interface areas are then calculated accordingly, e.g., using the relations discussed above and the geometric data of fractures and vugs. Once a proper mesh for a multiple-continuum system is generated, fracture, vuggy, and matrix blocks are specified, separately, to represent fracture or matrix continua.

In addition to discretization techniques discussed above, the following assumption may be also used: there is equilibrium within vugs, i, e., no flow calculations are needed within vugs.

Numerical Solution Scheme

There are a number of numerical solution techniques that have been developed in the literature over the past few decades to solve the nonlinear, discrete equations of reservoir simulations. When handling coupled flow, transport, and heat transfer in a subsurface system, the predominant approach is to use a fully implicit scheme. This scheme is best because of the extremely high nonlinearity inherent in those discrete equations and the many numerical schemes with different level of explicitness that fail to converge in practice. In this section, we discuss a general procedure to solve the discrete nonlinear Equation (12) fully implicitly, using a Newton iteration method.

Let us write the discrete nonlinear Equation (12) in a residual form as

$$R_i^{k,n+1} = \left\{M_i^{k,n+1} + G_i^{k,n+1} - M_i^{k,n}\right\}\frac{V_i}{\Delta t} - \sum_{j\in\eta_i} \text{flow}_{ij}^{k,n+1} - Q_i^{k,n+1} = 0 \qquad (33)$$

k = 1, 2, 3, …, N_c+1; i = 1, 2, 3, …, N).

Equation (33) defines a set of (N_c+1) × N coupled nonlinear equations that need to be solved for every balance equation of mass components and heat, respectively. In general, (N_c+1) primary variables per node are needed to use the Newton iteration for the associated (N_c+1) equations per node. The primary variables are usually selected among fluid pressures, mass (mole) fractions of components in fluids, and temperatures. The rest of the dependent variables, such as viscosity and densities, partitioning coefficients, specific enthalpies, thermal conductivities, dispersion tensor, as well as nonselected pressures and mass (mole) fractions—are treated as secondary variables, which are calculated from selected primary variables.

In terms of the primary variables, the residual equation, Equation (22), at a node i is regarded as a function of the primary variables at not only node i, but also at all its direct neighboring nodes j. The Newton iteration scheme gives rise to

$$\sum_m \frac{\partial R_i^{k,n+1}\left(x_{m,p}\right)}{\partial x_m}\left(\delta x_{m,p+1}\right) = -R_i^{k,n+1}\left(x_{m,p}\right) \qquad (34)$$

where x_m is the primary variable m with m = 1, 2, 3, …, N_c+1, respectively, at node i and all its direct neighbors; p is the iteration level; and i =1, 2, 3, …, N. The primary variables in Equation (34) need to be updated after each iteration:

$$x_{m,p+1} = x_{m,p} + \delta x_{m,p+1} \qquad (35)$$

The Newton iteration process continues until the residuals $R_n^{k,n+1}$ or changes in the primary variables $\delta x_{m,p+1}$ over an iteration are reduced below preset convergence tolerances.

Numerical methods are generally used to construct the Jacobian matrix for Equation (34), as outlined in Forsyth et al. (1995). At each Newton iteration, Equation (34) represents a system of (N_c+1) × N linearized algebraic equations with sparse matrices, which are solved by a linear equation solver.

Treatment of Initial and Boundary Conditions: A set of initial conditions is required to start a transient simulation, i.e., a complete set of primary variables need to be specified for every gridblock or node. A commonly used procedure for specifying initial conditions is the restart option, in which a complete set of initial conditions or primary unknowns is generated in a previous simulation, with proper boundary conditions described.

When using a block-centered grid, first-type or Dirichlet boundary conditions can be effectively treated with the "inactive cell" or "big-volume" method, as normally used in the TOUGH2 code (Pruess et al. 1999). In this method, a constant pressure/concentration/temperature node is specified as an inactive cell or with a huge volume, while keeping all the other geometric properties of the mesh unchanged. With finite-element or edge-centered finite-difference grids, first-type boundary conditions and Neuman boundary conditions can be treated using a generalized, sink/source term approach (Wu et al. 1996; Wu, 2000b). Certain flux-type boundary conditions are easy to handle for a situation in which flux distribution along the boundary is known, such as in dealing with surface infiltration. However, a description of more general types of flux or mixed boundaries, such as seepage faces and multilayered wells, is part of the solution, and general procedures for handling such boundary conditions are discussed in Wu et al. (1996).

Simulation Example

In this section, we demonstrate an application of the mathematic model discussed above. The reservoir simulator used is the modified TOUGH2 code – EOS3 (Pruess et al 1999) module with incorporation of density-dependent variation in water pressure or head. In the modeling studies, we use the modified TOUGH2-EOS3 to simulate nonisothermal flow of single-phase water with density dependence on mineral compositions in addition to pressure and temperature in the two wells, HDB-7 and HDB-8 at a Japanese site (JAEA, 2005). The two wells are located close to each other, but possibly separated by a fault.

The basic assumption in the modeling exercise is that the system is at steady state condition for water flow, solute transport, and heat flow. In particular, the aqueous mineral concentration distribution is assumed at steady state as a function of elevation or depth only for each well. Therefore, the water density is correlated to mineral compositions by extrapolating and interpolating the measured mineral compositional data from the two wells, in addition to its dependence to pressure and temperature. The two wells are represented using two 1-D column grids of 600 m with a uniform 5 m grid spacing, starting from zero depth at the ground surface using a single-continuum, multi-layered modeling approach. The geologic units/layers associated with the two 1-D models are shown in Tables 2 and 3, respectively, for Well HDB-7 and HDB-8. For Well HDB-7, the 1-D model grid starts from zero depth at the ground surface (elevation of 43.752 m) down to 600 m in depth, the geologic unit (Table 2) associated from 0 to 400 m is the Yuuch F. and from 400 m down belongs to Koetoi unit. For Well HDB-8, the 1-D model covers from the surface at an elevation of 70.051 m down to 600 m depth with the top layer of 140 m being the Koetoi unit, the unit below is the Wakkanai F (Table 3).

Table 4 lists the measured total mineral concentrations of the liquid water and depth data, as well as the calculated density factors used in the simulation to modify liquid densities. The porosity and permeability data for the well models are listed in Table 5. Note that the permeability values in Table 5 are converted using a constant liquid density of 1000.1 (kg/m^3) and a constant viscosity of 0.0011 (Pa•s).

A series of simulations for the two 1-D models are conducted as follows: Simulations with the hydrostatic condition are first carried out for determining top and bottom boundary conditions, in terms of pressures and temperatures, by matching the measured temperature and pressure data of Table 2 and 3. The results of the steady-state simulations are then used as base models for flow scenario analysis. Water is injected from top or bottom boundaries of the two well models with different injection rates. This is to estimate the localized downwards flow or upwards flow conditions, while keeping constant temperature data on both top and bottom boundaries.

In the literature (e.g., Wu et al. 2004; 2007a), geothermal gradients or temperature profiles are very sensitive to groundwater flow and useful in estimating water percolation fluxes in subsurface, Here, we use the measured temperature data to estimate both flow rate and flow directions at the two wells. Figures 4, 5, and 6 show comparisons between simulated temperature/pressures and the measurements for Well HDB-7. Figure 4 shows that at Well HDB-7, if we inject water from the bottom, i.e., water flows up, the simulated temperature data cannot match the measured values. However, if we inject water from the top, Figure 5 indicates the measured temperature could be fitted well at a flow rate of 3 mm/yr. Figure 6 presents pressure profiles simulated with water injection at top and indicates lower injection rates match measured pressure better. The difference between simulated and measured results in Figure 6 is primarily due to 1-D flow assumption in the model, while at the field condition, downwards flow will be subjected to multi-dimensional flow, find least flow resistance paths, and the top pressure would be lower.

Note that the two wells, HDB-7 and HDB-8, are close to each other, with HDB 8 being further inland. A comparison between the simulation results and measurements of temperature and pressures, discussed above, indicates different flow directions, i.e., flow at HDB-8 is upwards (discharge) and flow at HDB-7 is downwards (recharge). This indicates that there likely exists a fault separating the two wells and the fault behaves as a closed boundary or low-permeability barrier to flow across the fault between the two wells.

Figures 7, 8 and 9 show the results for Well HDB-8. For this well, Figure 7 shows that best estimated flow rate is at about 6 mm/yr, injected from the bottom boundary. This means upward flow at this location. If injected from the top, Figure 8 shows that simulated results cannot match the measured temperature profiles at all. Figure 9 shows the results and comparisons of pressures for upward flow, indicating a good agreement for a flow rate of 6 mm/yr.

Summary

A physically based conceptual and numerical model is presented for simulating fluid and heat flow and solute transport through fractured fault zones using a multiple-continuum medium approach. The suggested multiple-continuum concept is a natural extension of the classic double-porosity model, with the fracture continuum responsible for conducting global flow, while vuggy (if any) and matrix continua, locally connected and interacting with globally connecting fractures, provide storage space for fluid and solute.

The proposed conceptual model can be implemented into a general multidimensional numerical reservoir simulator TOUGH2 using a control-volume, finite-difference approach, which can be used to simulate single-phase flow, solute transport and heat transfer in 1-D, 2-D and 3-D fractured reservoirs. Model application is demonstrated for modeling two well flow problems at ambient geothermal and water flow condition.

Acknowledgments

This work was supported in part by Colorado School of Mines, by National Basic Research Program of China (973 Program), "Studying the Fundamentals of the Carbonate Karst Reservoir Development 2006CB202400", by Japan Atomic Energy Agency through the US Department of Energy under Contract No. DE-AC03-76SF00098.

References

1. Aziz, K. and A. Settari, *Petroleum Reservoir Simulation*, Applied Science Publishers LTD, London, 1979.
2. Barenblatt, G. I., Zheltov, I. P., and Kochina, I. N., Basic concepts in the theory of seepage of homogeneous liquids in fissured rocks, PMM, *Sov. Appl. Math. Mech.,* 24(5), 852–864, 1960.
3. Biot, M. A., General theory of three dimensional consolidation, *J. Appl Phys.*, 12:57-64, 1941.
4. Bird, R. B., W. E. Steward, E. N. Lightfoot. Transport Phenomena, John Willey & Sons, Inc., New York, London, Sydney, 1960.
5. Camacho-Velazquez, R., M. Vasquez-Cruz, R. Castrejon-Aivar, and V. Arana-Ortiz, Pressure transient and decline-curve behavior in naturally fractured vuggy carbonate reservoirs, *SPE Reservoir Evaluation & Engineering,* 95-111, April, 2005.
6. Closemann, P.J., The aquifer model for fissured fractured reservoir, *Soc. Pet. Eng. J.*, 385–398, 1975.
7. Forsyth, P. A., Y. S. Wu and K. Pruess, Robust numerical methods for saturated-unsaturated flow with dry initial conditions in heterogeneous media, *Advance in Water Resources,* 18, 25-38, 1995.
8. Forsyth, P. A., Three-dimensional modeling of steam flush for DNAPL site remediation, *International Journal for Numerical Methods in Fluids, Vol.* 19, 1055-1081, 1994.
9. Huyakorn, P. S., S. Panday and Y. S. Wu, "A three-dimensional multiphase flow model for assessing NAPL contamination in porous and fractured media, I. Formulation," *Journal of Contaminant Hydrology*, Vol. 16, 109-130, 1994.
10. JAEA, Horonobe URL Project, H16 Investigative Research Report, JNC TN5400 2005-001, 2005.
11. Kang, Zhijiang, Yu-Shu Wu, Jianglong Li, Yongchao Wu, Jie Zhang, and Guangfu Wang, Modeling multiphase flow in naturally fractured vuggy petroleum reservoirs, PSE-1-2356, Presented at the 2006 SPE Annual Technical Conference and Exhibition, San Antonio, Texas, 24-27 September, 2006.
12. Kazemi, H., Pressure Transient Analysis of Naturally Fractured Reservoirs with Uniform Fracture Distribution. *SPEJ,* 451–462. Trans., AIME, 246, 1969.
13. Liu, J. C. G. S. Bodvarsson, and Y. S. Wu, Analysis of pressure behavior in fractured lithophysal reservoirs, *Journal of Contaminant Hydrology*, 62-62, 189-211, 2003.
14. Narasimhan, T. N. and P. A. Witherspoon, An Integrated Finite difference method for analyzing fluid flow in porous media, *Water Resources Research, 12(1)*, 57-64, 1976.
15. Pan, L., C. Haukwa, Y. S. Wu, and G. S. Bodvarsson, "Development of WinGrider: An Interactive Grid Generator for TOUGH2," *Earth Sciences Division Annual Report, 1998-1999*, Lawrence Berkeley National Laboratory, LBNL-43816, pp.73-74, 2000.
16. Pruess K., Oldenburg, C., and Moridis, G., TOUGH2 User's Guide, Version 2.0, Report LBNL-43134, Berkeley, California: Lawrence Berkeley National Laboratory, 1999.
17. Pruess, K. and Narasimhan, T. N., A practical method for modeling fluid and heat flow in fractured porous media, *Soc. Pet. Eng. J.,* 25, 14-26, 1985.
18. Pruess, K., GMINC-A mesh generator for flow simulations in fractured reservoirs, Report LBL-15227, Berkeley, California: Lawrence Berkeley National Laboratory, 1983.
19. Scheidegger, A. E., General theory of dispersion in porous media, *J. Geophys. Res.,* Vol. 66, 3273-3278, 1961.
20. Snow, D. T., A parallel plate model of fractured permeable media, Ph.D. Dissertation, University of California, Berkeley, Californian, 1965.
21. Terzaghi, K., *Theoretical Soil Mechanics*, John Wiley & Sons Inc., New York, 1943.
22. Warren, J. E. and Root, P. J., The behavior of naturally fractured reservoirs, *Soc. Pet. Eng. J.,* 245–255, Trans., AIME, 228, 1963.

23. Wu, Y. S., J. Rutqvist, K. Karasaki, Q. Lei, W. Xiong, J. Yuan, J., and M. Liu, A mathematical model for rock deformation's effects on flow in porous and fractured reservoirs, prepared for presentation at San Francisco 2008, the 42nd US Rock Mechanics Symposium and 2nd U.S.-Canada Rock Mechanics Symposium, held in San Francisco, June 29-July 2, 2008.
24. Wu, Yu-Shu, Guoping Lu, Keni Zhang, L. Pan, and G. S. Bodvarsson, "Analyzing Unsaturated Flow Patterns in Fractured Rock Using an Integrated Modeling Approach," LBNL-54006, *Hydrogeology Journal*, Vol. 15, pp.553-572, 2007a.
25. Wu, Yu-Shu, Christine Ehlig-Economides, Guan Qin, Zhijiang Kang, Wangming Zhang Babatunde Ajayi, and Qingfeng Tao, "A Triple Continuum Pressure Transient Model for A Naturally Fractured Vuggy Reservoir," SPE-110044, presented at the 2007 SPE Annual Technical Conference and Exhibition held in Anaheim, California, 11–14 November 2007b.
26. Wu, Yu-Shu, S. Mukhopadhyay , K. Zhang, and G. S. Bodvarsson, "A Mountain-Scale Thermal-Hydrologic Model for Simulating Fluid Flow and Heat Transfer in Unsaturated Fractured Rock," LBNL-57921, *Journal of Contaminant Hydrology,* Vol. 86, pp.128-159, 2006a.
27. Wu, Y. S., G. Qin, Richard E. Ewing, Yalchin Efendiev, Zhijiang Kang and Yulin Ren, "A Multiple-Continuum Approach for Modeling Multiphase Flow in Naturally Fractured Vuggy Petroleum Reservoirs," SPE-104173, Presented at the 2006 SPE International Oil & Gas Conference and Exhibition, Beijing, China, 5–7 December, 2006b.
28. Wu, Y. S., G. Lu, K. Zhang, and G. S. Bodvarsson, "A Mountain-Scale Model for Characterizing Unsaturated flow and Transport in Fractured Tuffs of Yucca Mountain," LBNL-52524, *Vadose Zone Journal*, Vol. 3, pp.796-805, 2004.
29. Wu, Y. S., H. H. Liu, And G. S. Bodvarsson, A triple-continuum approach for modeling flow and transport processes in fractured rock, *Journal Of Contaminant Hydrology*, 73, 145-179, 2004a.
30. Wu, Y. S., A unified numerical framework model for simulating flow, transport, and heat transfer in porous and fractured media, *Developments In Water Science,* Edited By Cass T. Miller, Matthew W. Farthing, William G. Gray, And George F. Pinder, Elsevier, 2004b.
31. Wu, Y. S., Numerical simulation of single-phase and multiphase non-Darcy flow in porous and fractured reservoirs, *Transport In Porous Media*, Vol. 49, No. 2, pp.209-240, 2002.
32. Wu, Y. S., On the effective continuum method for modeling multiphase flow, multicomponent transport and heat transfer in fractured rock, Book chapter of "*Dynamics of Fluids in Fractured Rocks, Concepts and Recent Advances*", Edited by B. Faybishenko, P. A. Witherspoon and S. M. Benson, AGU Geophysical Monograph 122, American Geophysical Union, Washington, DC, 299–312, 2000.
33. Wu, Y. S. and K. Pruess, Numerical simulation of non-isothermal multiphase tracer transport in heterogeneous fractured porous media, *Advance in Water Resources*, 23, 699-723, 2000a.
34. Wu, Y. S., A virtual node method for handling wellbore boundary conditions in modeling multiphase flow in porous and fractured media, *Water Resources Research*, 36 (3), 807-814, 2000b.
35. Wu, Y. S., P. A. Forsyth and H. Jiang, A consistent approach for applying numerical boundary conditions for subsurface flow, *Journal of Contaminant Hydrology*, Vol. 23, 157-185, 1996.
36. Wu, Y. S. and Pruess K., A multiple-porosity method for simulation of naturally fractured petroleum reservoirs, *SPE Reservoir Engineering*, 3, 327-336, 1988.

Table 1. Characteristic distances* for evaluating flow terms between fractures, vugs, and matrix systems

Fracture Sets	Dimensions of Matrix Blocks (m)	Characteristic F-M Distances (m)	Characteristic F-V Distances (m)	Characteristic V-M Distances [1] (m)	Characteristic V-M Distances [2] (m)
1-D	A	$l_{FM} = A/6$	$l_{FV} = l_x$	$l_{VM} = a/6$	$l_{VM} = (A - d_c)/2$
2-D	A, B	$l_{FM} = AB/4(A+B)$	$l_{FV} = \frac{l_x + l_y}{2}$	$l_{VM} = ab/4(a+b)$	$l_{VM} = \frac{A+B-2d_c}{4}$
3-D	A, B, C	$l_{FM} = 3ABC/10/(AB+BC+CA)$	$l_{Ff} = \frac{l_x + l_y + l_z}{3}$	$l_{VM} = 3abc/10/(ab+bc+ca)$	$l_{Ff} = \frac{A+B+C-3d_c}{6}$

* Note in Table 3.1, A, B, and C are dimensions of matrix blocks along x, y, and z directions, respectively.
[1] Characteristic V-M distances are estimated for the case that vuggy-matrix connections are dominated by small fractures, where dimensions a, b, and c are fracture-spacings of small fractures along x, y, and z directions, respectively.
[2] Characteristic V-M distances are used for the case that vugs are isolated from fractures.

Table 2. Geologic units/layers and measured temperature and pressure data for Well HDB-7

Geologic Units/Layers	Depth (m)	Thickness (m)	Temperature (°C)	Pressure (KPa)
Yuuchi F.	45.35	97.71	8.55	549.27
Yuuchi F.	143.06	48.74	12.2	1600.14
Yuuchi F.	191.80	15.26	14.11	2099.64
Yuuchi F.	207.06	15.04	14.62	2259.53
Yuuchi F.	222.09	10.76	15.13	2414.1
Yuuchi F.	232.86	98.02	15.55	2529.13
Yuuchi F.	330.88	25.77	19.53	3522.07
Yuuchi F./Koetoi F.	356.64	91.53	20.56	3790.36
Koetoi F.	448.17	75.33	24.51	4709.45

Table 3. Geologic units/layers and measured temperature and pressure data for Well HDB-8

Geologic Units/Layers	Depth (m)	Thickness (m)	Temperature (°C)	Pressure (KPa)
Koetoi F.	65.48	31.74	31.74	680.89
Koetoi F.	97.22	10.75	10.75	996.56
Koetoi F./Wakkanai F.	107.97	69.01	69.01	1103.02
Wakkanai F.	176.98	29.75	29.75	1784.73
Wakkanai F.	206.73	73.74	73.74	2077.55
Wakkanai F.	280.43	10.72	10.72	2734.68
Wakkanai F.	291.15	100.48	100.48	2938.81
Wakkanai F.	391.64	49.5	49.5	3944.4
Wakkanai F.	441.13	32.33	32.33	4433.35

Table 4. Measured total mineral concentrations and calculated density factors used for modifying water density as a function of total concentrations ort depth

Well	Depth (m)	Total concentration (ppm)	Density factor
HDB-7	41.61	4,698	1.003
HDB-7	131.13	9,928	1.008
HDB-7	320.52	29,107	1.027
HDB-7	343.42	31,572	1.030
HDB-7	398.90	28,850	1.027
HDB-7	442.20	31,094	1.029
HDB-7	496.25	28,440	1.026
HDB-7	506.64	29,230	1.027
		-	
HDB-8	63.15	3,255	1.001
HDB-8	101.87	4,204	1.002
HDB-8	283.82	11,469	1.009
HDB-8	344.45	12,395	1.010
HDB-8	400.79	12,014	1.010
HDB-8	449.14	13,066	1.011
HDB-8	465.34	15,175	1.013

Table 5. Permeability and porosity values for different geologic units/layers

Geologic Unit	Hydraulic conductivity (m/sec)	Permeability (m^2)	Porosity
Quaternery Sediments	1.00E-06	1.10E-13	0.55
Yuuchi F.	5.70E-10	6.27E-17	0.55
Koetoi F.	3.59E-09	3.95E-16	0.55
Wakkanai F.	1.36E-08	1.50E-15	0.45
Masuhoro F.	5.00E-10	5.50E-17	0.4
Cretaceous rock	1.00E-11	1.10E-18	0.4
Fault	1.00E-10	1.10E-17	0.55

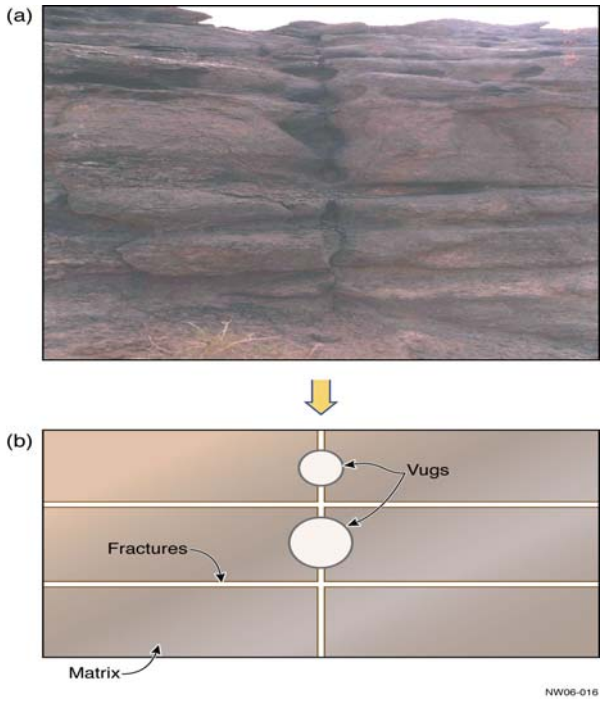

Figure 1. Schematic of conceptualizing vuggy fractured formation as a discrete fracture system with well connected, (a) outcrop pictures and (b) conceptual model (Wu et al. 2006).

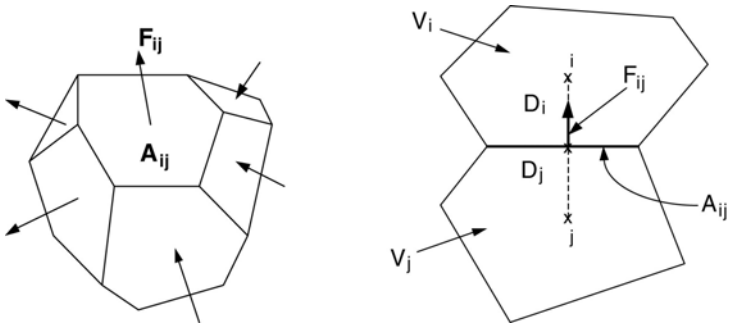

Figure 2. Space discretization and flow-term evaluation in the integral finite difference method (Pruess et al. 1999).

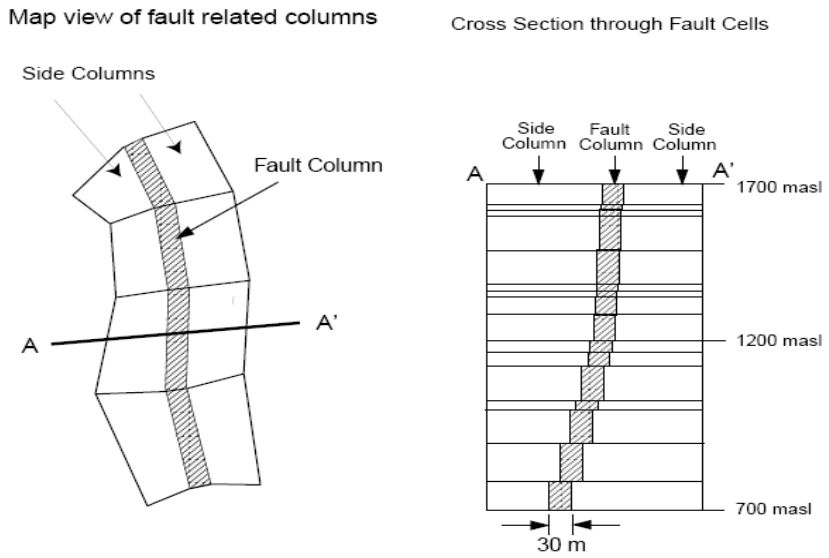

Figure 3. Handling three-dimensional faults and fault zones using the Windridder-TOUGH2 methodology (Pan et al. 2000).

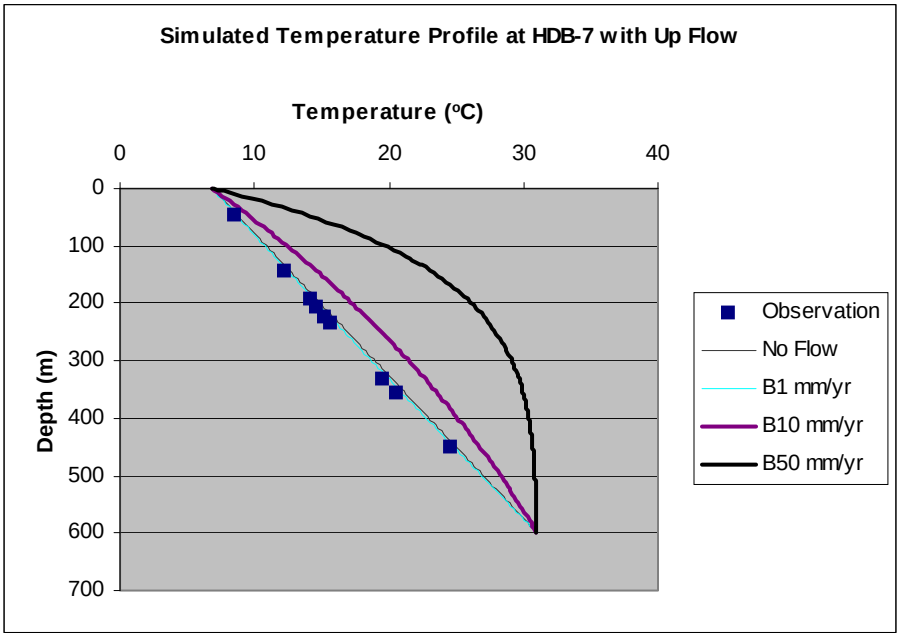

Figure 4. Comparison of simulated and measured temperatures at Well HDB-7 with water injected at bottom boundary at a rate of 0, 1 mm/yr, 10/mmyr, and 50 mm/yr.

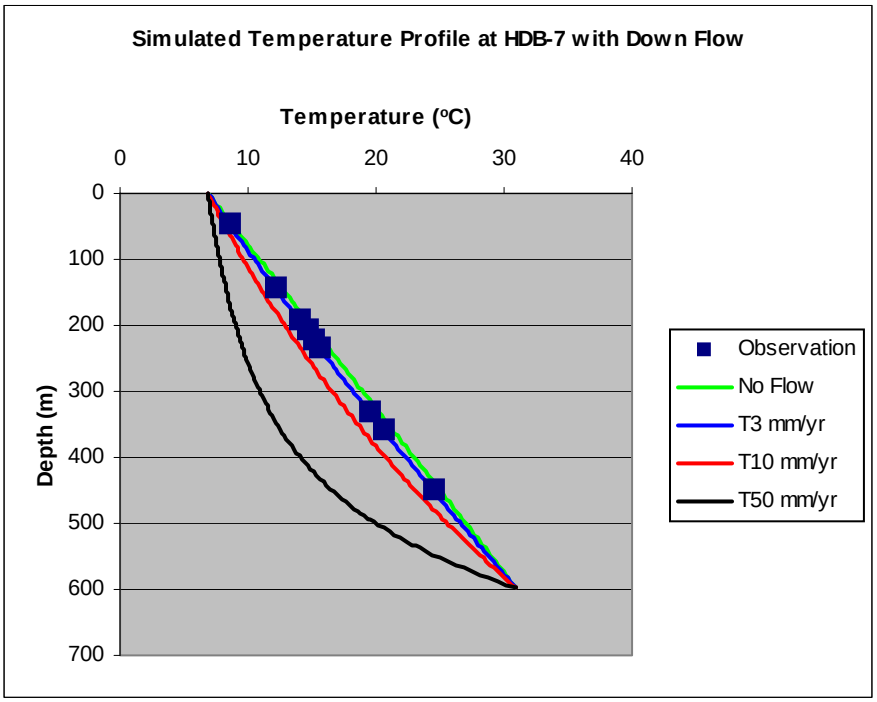

Figure 5. Comparison of simulated and measured temperatures at Well HDB-7 with water injected at top boundary at a rate of 0, 3 mm/yr, 10/mmyr, and 50 mm/yr.

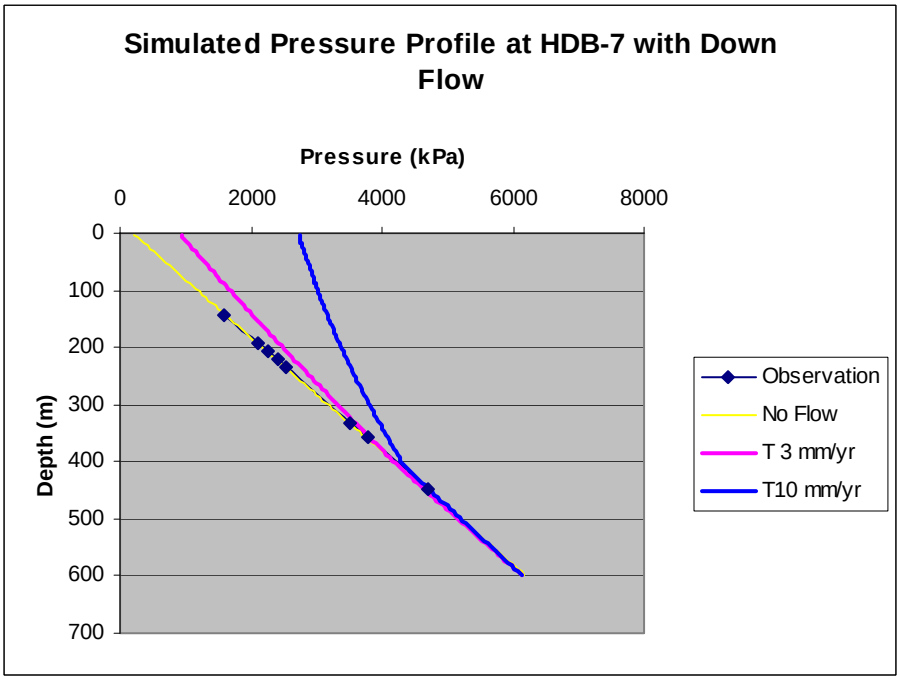

Figure 6. Comparison of simulated and measured pressures at Well HDB-7 with water injected at top boundary at a rate of 0, 3 mm/yr, and 10/mmyr.

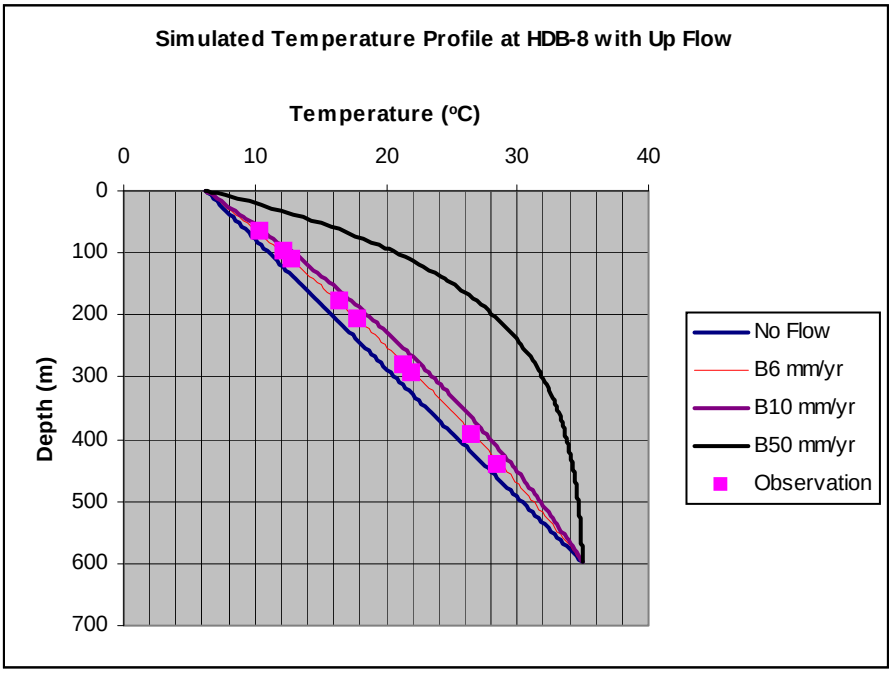

Figure 7. Comparison of simulated and measured temperatures at Well HDB-8 with water injected at bottom boundary at a rate of 0, 6 mm/yr, 10/mmyr, and 50 mm/yr.

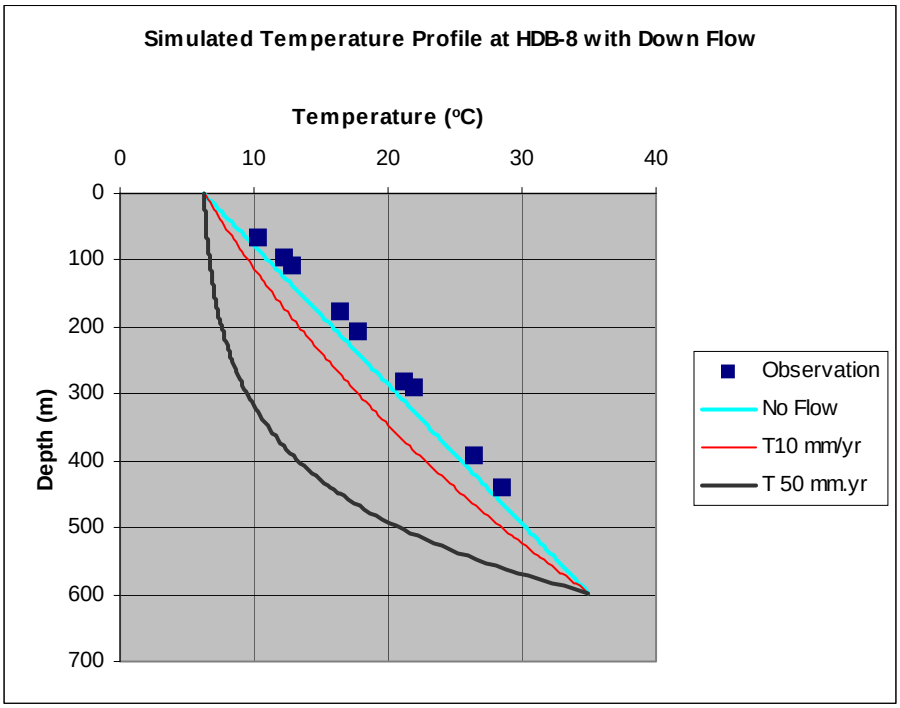

Figure 8. Comparison of simulated and measured temperatures at Well HDB-8 with water injected at top boundary at a rate of 0, 10 mm/yr, and 50 mm/yr.

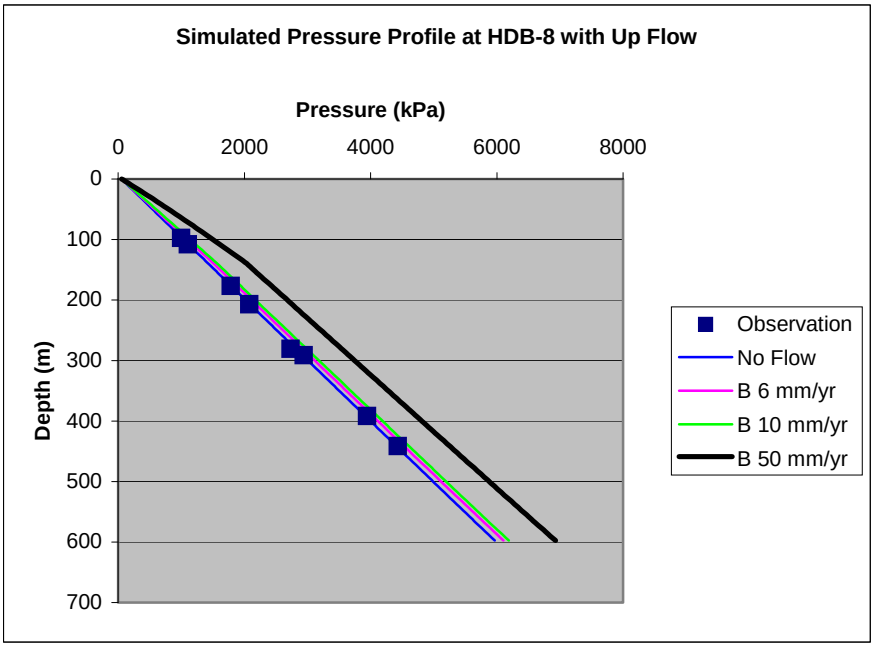

Figure 9. Comparison of simulated and measured pressures at Well HDB-8 with water injected at bottom boundary at a rate of 0, 6 mm/yr, 10/mmyr, and 50 mm/yr.